Journal of Biomolecular NMR, 7 (1996) 261–272
ESCOM

J-Bio NMR 341

^{19}F NMR relaxation studies on 5-fluorotryptophan- and tetradeutero-5-fluorotryptophan-labeled *E. coli* glucose/galactose receptor

Linda A. Luck*, Joseph E. Vance, Thomas M. O'Connell** and Robert E. London***

Laboratory of Molecular Biophysics, National Institute of Environmental Health Sciences, National Institutes of Health, P.O. Box 12233, Research Triangle Park, NC 27709, U.S.A.

Received 16 August 1995
Accepted 15 February 1996

Keywords: Glucose/galactose receptor; GGR; ^{19}F NMR; Fluorotryptophan; Protein dynamics

Summary

^{19}F NMR relaxation studies have been carried out on a fluorotryptophan-labeled *E. coli* periplasmic glucose/galactose receptor (GGR). The protein was derived from *E. coli* grown on a medium containing a 50:50 mixture of 5-fluorotryptophan and [2,4,6,7-$^2H_4$]-5-fluorotryptophan. As a result of the large γ-isotope shift, the two labels give rise to separate resonances, allowing relaxation contributions of the substituted indole protons to be selectively monitored. Spin-lattice relaxation rates were determined at field strengths of 11.75 T and 8.5 T, and the results were analyzed using a model-free formalism. In order to evaluate the contributions of chemical shift anisotropy to the observed relaxation parameters, solid-state NMR studies were performed on [2,4,6,7-$^2H_4$]-5-fluorotryptophan. Analysis of the observed ^{19}F powder pattern lineshape resulted in anisotropy and asymmetry parameters of $\Delta\sigma = -93.5$ ppm and $\eta = 0.24$. Theoretical analyses of the relaxation parameters are consistent with internal motion of the fluorotryptophan residues characterized by order parameters S^2 of ~1, and by correlation times for internal motion ~ 10^{-11} s. Simultaneous least squares fitting of the spin-lattice relaxation and line-width data with τ_i set at 10 ps yielded a molecular correlation time of 20 ns for the glucose-complexed GGR, and a mean order parameter $S^2 = 0.89$ for fluorotryptophan residues 183, 127, 133, and 195. By contrast, the calculated order parameter for FTrp^{284}, located on the surface of the protein, was 0.77. Significant differences among the spin-lattice relaxation rates of the five fluorotryptophan residues of glucose-complexed GGR were also observed, with the order of relaxation rates given by: $R_{1F}^{183} > R_{1F}^{127} \sim R_{1F}^{133} \sim R_{1F}^{195} > R_{1F}^{284}$. Although such differences may reflect motional variations among these residues, the effects are largely predicted by differences in the distribution of nearby hydrogen nuclei, derived from crystal structure data. In the absence of glucose, spin-lattice relaxation rates for fluorotryptophan residues 183, 127, 133, and 195 were found to decrease by a mean of 13%, while the value for residue 284 exhibits an increase of similar magnitude relative to the liganded molecule. These changes are interpreted in terms of a slower overall correlation time for molecular motion, as well as a change in the internal mobility of FTrp^{284}, located in the hinge region of the receptor.

Introduction

^{19}F NMR is increasingly used to probe structural and conformational features of proteins too large for ^{1}H NMR analysis (Gerig, 1994, and references cited therein). Typically, such proteins are grown on media containing fluorinated amino acids, although other fluorination strategies have also been used. Despite early concerns about the significance of chemical shift anisotropy relaxation mechanisms for fluorinated macromolecules, surprisingly well-resolved spectra have often been obtained at fields up to 11.75 T (Luck and Falke, 1991a–c; Hoeltzli and Frieden, 1994) and for high molecular weights (Hull and Sykes, 1974,1975b; Browne and Otvos, 1976; Gerig et al., 1983;

*Present address: Department of Biology, Science Center, Clarkson University, Potsdam, NY 13669, U.S.A.
**Present address: Laboratory of Molecular Modeling, School of Pharmacy CB #7360, University of North Carolina, Chapel Hill, NC 27514, U.S.A.
***To whom correspondence should be addressed.

Abbreviations: FTrp, D,L-5-fluorotryptophan; GGR, glucose/galactose receptor protein; R_{1F}, spin-lattice relaxation rate of fluorine; $R_{1F}(H)$, spin-lattice relaxation rate of the fluorine nuclei in normal (nondeuterated) fluorotryptophan residues; $R_{1F}(D)$, spin-lattice relaxation rate of the fluorine in [2,4,6,7-$^2H_4$]-5-fluorotryptophan.

Peersen et al., 1990; Hinds et al., 1992). In order to develop optimal labeling strategies and to characterize molecular dynamics, additional characterization of the relaxation behavior of fluorinated macromolecules would be useful. As initially demonstrated by Moreland and Carroll (1974), the measurement of the relaxation rates for simultaneously observed molecular isotopomers can provide unique insights into molecular dynamics and relaxation mechanisms. In such studies, all physical parameters for the different isotopically labeled species are identical, except for the interactions that vary with the isotopic species being observed. No analyses of this type appear to have been done for fluorine, presumably due to the difficulty of simultaneously introducing ^{13}C and ^{19}F labels, and to the fact that no other primary isotope effect would be achievable.

In this paper, we note that γ-isotope effects resulting from deuteration of vicinal protons are sufficiently large to permit the separation of ^{19}F resonances, even in relatively large macromolecular systems. We have utilized this strategy with the glucose/galactose periplasmic receptor protein of *E. coli*, a soluble protein of MW = 33 370. Previous studies by Luck and Falke (1991a–c) show that the resonances corresponding to the five fluorotryptophan residues of 5FTrp-labeled GGR are well resolved, particularly for the glucose-ligated form of the receptor. The labeling protocol involves growth of the protein on a medium containing equal concentrations of 5-fluorotryptophan and [2,4,6,7-$^2H_4$]-5-fluorotryptophan. This approach provides a theoretical basis for the separation of intraresidue and interresidue contributions to the relaxation parameters. Field-dependent relaxation measurements and solid-state NMR studies have been performed in order to obtain a better understanding of tryptophan dynamics.

Materials and Methods

D,L-5-fluorotryptophan was obtained from Sigma (St. Louis, MO). The [2,4,6,7-$^2H_4$]-D,L-5-fluorotryptophan was either obtained from Isotec, Inc. (Miamisburg, OH), or was prepared using published procedures (Griffiths et al., 1976; Matthews et al., 1977) for tryptophan deuteration. The techniques used to generate and isolate the FTrp-labeled receptor have been described previously (Luck and Falke, 1991a), the only modification being the substitution of a 50:50 mixture of the D,L-5-fluorotryptophan and [2,4,6,7-$^2H_4$]-D,L-5-fluorotryptophan in the growth medium.

^{19}F NMR measurements were done on the purified enzyme in a buffer containing 10% D_2O for the deuterium lock, 0.5 mM $CaCl_2$, 100 mM KCl, and 10 mM Tris-HCl, pH 7.1. ^{19}F spectra at 470 MHz were obtained on a GN-500 NMR spectrometer (GE NMR, Fremont, CA), and 340 MHz spectra were obtained on an NT-360 spectrometer (Nicolet Magnetics Corp., Fremont, CA). All NMR studies were performed at 25 °C. The R_{1F} values summarized in the tables are averages of two separate determinations, and the variation was generally < 10%. In several cases, measurements were repeated 3–4 times on different enzyme preparations, and standard deviations ranged from 5 to 16%. T_1 measurements were done using an inversion-recovery sequence. In order to investigate the possible interconversion between folded and denatured enzyme, the fluorine resonance(s) of the latter were selectively inverted using a DANTE pulse sequence (Morris and Freeman, 1978). CHARMm calculations were performed on a Silicon Graphics Indigo XS-4000 workstation.

Initially, dynamic variables were estimated assuming rigid, isotropic motion of the glucose–GGR complex. Subsequently, dipolar and chemical shift anisotropy contributions to the ^{19}F relaxation of the fluorotryptophan-labeled complex were modeled using a 'model-free' spectral density formalism (Lipari and Szabo, 1982), and the ranges of dynamic variables consistent with the observed relaxation parameters were determined. Finally, dynamic variables were optimized by minimizing an error function defined as the sum of the squares of the fractional differences between calculated and experimental relaxation parameters:

$$\text{Error} = \sum_i [(P_i^{exp} - P_i^{calc}) / P_i^{exp}]^2 \qquad (1)$$

The relaxation contributions of the indole protons were isolated by measurements of the relaxation-rate differences between the protonated and deuterated fluorotryptophan residues. Using the abbreviation $R_{1F}(i)^{\nu}$ for the fluorine spin-lattice relaxation rate in the 5-fluorotryptophan (i = H) or deuterated 5-fluorotryptophan (i = D) residues at NMR frequency ν (in MHz), the three parameters used in the minimization were $R_{1F}(H)^{470} - R_{1F}(D)^{470}$, $R_{1F}(H)^{340} - R_{1F}(D)^{340}$, and the CSA line-width contribution, $W_{1/2}^{CSA}$. Since the resulting error function was found to be fairly insensitive to the value of τ_i, the correlation time for internal motion, for values near 10 ps, τ_i was fixed at this value and only the molecular correlation time, τ_M, and the order parameter, S^2, were varied in the minimization.

Solid-state ^{19}F NMR spectra of a powder sample of [2,4,6,7-$^2H_4$]-D,L-5-fluorotryptophan were performed on a Varian UnityPlus 500 MHz spectrometer at 25 °C using a spin-echo pulse sequence. To ensure constant excitation over the fluorine bandwidth, short rf pulse lengths of 2 and 4 μs were used. Such an approach minimizes distortion due to the finite pulse power (Rance and Byrd, 1983). A total of 360 FIDs were averaged, left-shifted three times to center the echo about the time origin, and phased such that the real and imaginary components were purely absorptive and dispersive, respectively. A 1-kHz exponential line-broadening was applied prior to Fourier transformation. Theoretical solid-state powder spectra were

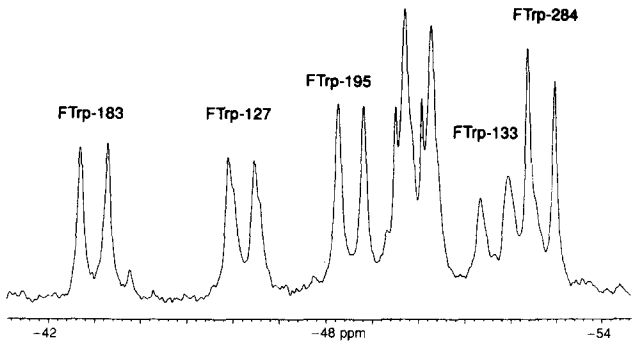

Fig. 1. ^{19}F NMR spectrum (470 MHz) of the *E. coli* glucose/galactose receptor (GGR) grown on a medium containing a 50:50 mixture of 5-fluorotryptophan and [2,4,6,7-$^2H_4$]-5-fluorotryptophan. The spectrum corresponds to the GGR–glucose complex. The resonances corresponding to $FTrp^{127}$ and $FTrp^{133}$ show additional splitting due to a slow conformational exchange process. This splitting is not well resolved for $FTrp^{127}$, while for $FTrp^{133}$ the splitting is 0.65 ppm. Hence, the $FTrp^{133}$ resonances actually appear as three resolved signals, with the component furthest upfield overlapping one of the $FTrp^{284}$ resonances. The resonances marked with an asterisk correspond to denatured protein, while other minor peaks arise due to complexation of the GGR with small amounts of sugars other than glucose. Other sample parameters are: [GGR] = 1.2 mM, T = 25 °C, 10% D_2O for the deuterium lock, 0.5 mM $CaCl_2$, 100 mM KCl, and 10 mM Tris-HCl, pH 7.1.

generated by the convolution of the lineshape function generated as described by Mehring (1976) with a Gaussian function, using a program written in MATHEMATICA.

Results

The *E. coli* GGR consists of two domains which come together to form the sugar binding pocket (Vyas et al., 1988). It contains five tryptophan residues at positions 127, 133, 183, 195, and 284. Trp^{183} is located in the binding pocket on the surface of one of the domains, so that it is in van der Waals contact with the D-glucose upon binding. Trp^{127} and Trp^{133} are located at the base of the calcium-ion binding site, and are split into two resonances, presumably as a consequence of conformational heterogeneity, which is slow on the NMR time scale. The proton-coupled ^{19}F NMR spectrum of the GGR–glucose complex grown on a medium containing a 50:50 mixture of D,L-5-fluorotryptophan and [2,4,6,7-$^2H_4$]-D,L-5-fluorotryptophan is shown in Fig. 1. The glucose complex was selected for analysis due to the considerably better resolution of the tryptophan resonances in this state. As is apparent from this figure, each of the fluorine resonances which appear in the ^{19}F NMR spectrum of the 5-fluorotryptophan-labeled enzyme (Luck and Falke, 1991a) is now doubled. The observed isotope-shift value of –0.58 ppm is approximately double the value of –0.262 ppm, which has been reported for each *ortho*-deuterium substitution in the [3,5-$^2H_2$]-4-fluorobenzenesulfonyl fluoride (Ando et al., 1986), and is also consistent with the γ-deuterium isotope shifts observed in fluoroethanes (Osten et al., 1985). The resonances due to $FTrp^{133}$ now appear as three separate peaks due to the combined effects of the conformational shift ($\Delta\nu = 0.65$ ppm) and the isotope shift, with the resonance furthest upfield overlapping one of the $FTrp^{284}$ resonances.

Since a significant fraction of the protein in these samples was found to be denatured, the possible significance of exchange between the folded and unfolded forms of the GGR was investigated using magnetization transfer. The resonance corresponding to the denatured fluorotryptophan-labeled GGR was selectively inverted using a DANTE pulse sequence (Morris and Freeman, 1978), and a series of spectra were obtained after a variable time period during which magnetization transfer could take place. No significant intensity variations for the resonances of the glucose-complexed GGR were observed, indicating that any possible interconversion between the folded and unfolded GGR occurs at rates much slower than the fluorine spin-lattice relaxation rate of the denatured protein (1.23 s^{-1}).

It is in principle possible that the substitution of a fluorotryptophan residue by a tryptophan residue could significantly destabilize the protein. If this were the case, it might be expected that such a destabilization effect would be position-dependent, with the result that the fluorotryptophan substitution level at the different positions would vary considerably. Three separate measurements performed on two different GGR samples yielded intensity ratios of 19%:23%:20%:19%:19% for 5FTrp residues 183:127:195:133:284, with the standard deviation for each below 2%. Hence, there appears to be a marginally greater labeling at position 127, but in general, no large variations are observed.

Spin-lattice relaxation rates for the resolved resonances of the fluorotryptophan/deuterated fluorotryptophan-labeled enzyme were determined at 470 MHz and at 340 MHz using standard inversion-recovery sequences. Although cross-relaxation effects would be expected to lead to nonexponential spin-lattice relaxation, the data fit well to single-exponential recovery curves. The relaxation rates are summarized in Table 1. From these data, several trends are apparent: (i) $FTrp^{127}$, $FTrp^{133}$, and $FTrp^{195}$

TABLE 1
^{19}F SPIN-LATTICE RELAXATION RATES OF FLUOROTRYPTOPHAN RESIDUES IN THE *E. coli* GLUCOSE/GALACTOSE RECEPTOR

Residue	$R_{1F}(H)^{470}$	$R_{1F}(D)^{470}$	Δ	$R_{1F}(H)^{340}$	$R_{1F}(D)^{340}$	Δ
$FTrp^{183}$	1.91	1.51	0.40	3.44	2.92	0.52
$FTrp^{127}$	1.34	0.91	0.43	2.80	1.72	1.08
$FTrp^{195}$	1.40	0.95	0.45	2.77	1.75	1.02
$FTrp^{133}$	1.35	1.07	0.28	2.26	1.72	0.54
$FTrp^{284}$	0.95	0.57	0.38	1.67	1.01	0.66
Average[a]	–	–	0.39	–	–	0.79

[a] Without $FTrp^{284}$.

TABLE 2
LINE WIDTHS OF RESOLVED TRYPTOPHAN RESONANCES

Residue	$W_{1/2}$ [a]	$W_{1/2}$ [b]	$W_{1/2}$ [c]
$FTrp^{183}$ H	60	25.6	34
D	54	19.1	35
$FTrp^{127}$ H	53	17.0	36
D	46	10.0	36
$FTrp^{195}$ H	62	19.9	42
D	55	13.2	42
$FTrp^{284}$ H	39	9.6	29
D	29	3.1	26

[a] Mean line widths (in Hz) at 470 MHz after subtraction of the 25-Hz exponential broadening function. The mean standard deviation was 15%.

[b] Theoretical dipolar contribution based on crystal-structure distances, including protons within 5 Å of the fluorine nuclei, and assuming $\tau_M = 23$ ns, no internal motion.

[c] After subtraction of the theoretical dipolar contribution.

exhibit similar relaxation rates, while $FTrp^{183}$ exhibits significantly greater relaxation rates, and $FTrp^{284}$ exhibits significantly lower relaxation rates; (ii) the relaxation rates are significantly higher at the lower field strength. Using the abbreviation $R_{1F}(i)^{\nu}$ for the fluorine spin-lattice relaxation rate in the 5-fluorotryptophan (i = H) or deuterated 5-fluorotryptophan (i = D) residues at NMR frequency ν (in MHz), the ratio $R_{1F}(H)^{340}/R_{1F}(H)^{470}$ averaged for each residue is 1.86 ± 0.17. The corresponding $R_{1F}(D)^{340}/R_{1F}(D)^{470} = 1.81 \pm 0.13$, so that the ratio determined at the two field strengths is not significantly changed by deuteration; (iii) the relaxation rate difference between the protonated and deuterated fluorotryptophans, which is theoretically the simplest parameter to interpret, has mean values of 0.39 s^{-1} and 0.79 s^{-1} at 11.75 T and 8.5 T, respectively, where the $FTrp^{284}$ values have not been included in the average, as discussed below; (iv) a comparison of the $R_{1F}(H)$ values and the $R_{1F}(H) - R_{1F}(D)$ values indicates that, although the intraresidue indole protons make a significant contribution to the observed relaxation, the dominant dipolar relaxation contribution arises from interactions with protons on other residues; and (v) the observed line widths are remarkably narrow, given the high field strength used and the expectation of significant broadening due to chemical shift anisotropy.

The ^{19}F spectra of 5FTrp-labeled GGR demonstrate the feasibility of obtaining useful spectroscopic data for relatively large proteins at high field strengths. The line widths of the well-resolved resonances are summarized in Table 2. After subtraction of the 25-Hz exponential broadening, line widths in the range of 46–62 Hz are obtained for $FTrp^{183}$, $FTrp^{127}$, and $FTrp^{195}$, while narrower resonances are observed for $FTrp^{284}$. Dipolar contributions to the line width at half height, $W_{1/2}$, calculated on the basis of the crystal structure as discussed below, have also been determined in order to consider more quantitatively the CSA broadening contributions.

Molecular correlation time

Assuming isotropic diffusion and no significant internal motion of fluorotryptophan residues 127, 133, 183, and 195, the average $R_{1F}(H) - R_{1F}(D)$ value of 0.39 s^{-1} at 500 MHz corresponds to a correlation time for overall molecular tumbling of $\tau_M = 24$ ns. The underlying calculations are discussed below in greater detail. The analogous difference of 0.79 s^{-1} measured at 340 MHz corresponds to a similar $\tau_M = 22$ ns. Assuming $\tau_M \propto$ MW, these values are in good agreement with the available literature. For example, rotational correlation times of 76 ns for alkaline phosphatase (T = 28 °C, MW = 86 000; Hull and Sykes, 1975b), and 9.3 ns for FK binding protein (T = 30 °C, MW = 11 800; Cheng et al., 1994) would correspond to τ_M values of 29 and 26 ns, respectively, for a protein of MW = 33 370. The rotational correlation time can also be derived from the field-dependent R_1 ratios: $R_{1F}(H)^{340}/R_{1F}(H)^{470}$ and $R_{1F}(D)^{340}/R_{1F}(D)^{470}$. Assuming only dipolar relaxation and isotropic motion, setting $\tau_M = 23$ ns (= 1/2(22 ns + 24 ns)) corresponds to a ratio of 1.83, which agrees well with the values obtained for either the protonated or deuterated fluorotryptophan residues, as noted above. Further refinement of the dynamic variables was performed as discussed below.

Dipolar contributions to the relaxation rates

Although ^1H-^{19}F cross-relaxation effects should in principle lead to nonexponential relaxation, the spin-lattice relaxation behavior for the fluorine nuclei was found to approximate reasonably an exponential recovery curve. Theoretical simulations using a heteronuclear relaxation-matrix treatment were performed in order to evaluate this

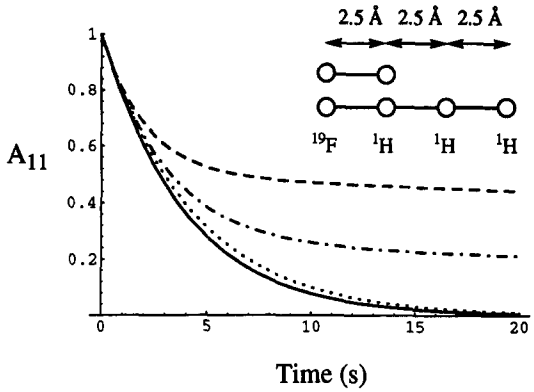

Fig. 2. Theoretical calculations of the spin-lattice relaxation behavior for a proton–fluorine heteronuclear spin system. The calculations correspond to the diagonal elements of a NOESY matrix, so that the relaxation behavior is normalized to decay from 1.0 to 0, nucleus 1 is ^{19}F, and nuclei 2 through n are ^1H. Calculations correspond to an isolated proton–fluorine spin pair at a distance of 2.5 Å (– – –), to four spins in a line with internuclear distances of 2.5 Å, with the first spin corresponding to ^{19}F, as shown in the inset (– · –), to the four-spin system with an additional relaxation sink of 1 s^{-1} added to the relaxation matrix for each proton spin (· · · ·), and finally to an exponential decay corresponding to $e^{-R_{11}t}$, where R_{11} is the first element of the relaxation matrix (——).

behavior more fully. The elements of the relaxation matrix are derived from the relations:

$$\rho_{HF} = \frac{2}{15}\frac{\gamma_H^2\gamma_F^2\hbar^2}{r_{HF}^6}s_H(s_H+1)[\,J(\omega_F-\omega_H)+3J(\omega_F)+6J(\omega_F+\omega_H)\,]$$

$$\rho_{DF} = \frac{2}{15}\frac{\gamma_D^2\gamma_F^2\hbar^2}{r_{DF}^6}s_D(s_D+1)[\,J(\omega_F-\omega_D)+3J(\omega_F)+6J(\omega_F+\omega_D)\,] \quad (2)$$

$$\rho_{H_iH_j} = \frac{2}{15}\frac{\gamma_H^4\hbar^2}{r_{H_iH_j}^6}s_H(s_H+1)[J(0)+3J(\omega_H)+6J(2\omega_H)]$$

$$\sigma_{HF} = \frac{2}{15}\frac{\gamma_H^2\gamma_F^2\hbar^2}{r_{HF}^6}s_H(s_H+1)[6J(\omega_H+\omega_F)-J(\omega_H-\omega_F)]$$

$$\sigma_{H_iH_j} = \frac{2}{15}\frac{\gamma_H^4\hbar^2}{r_{H_iH_j}^6}s_H(s_H+1)[6J(2\omega_H)-J(0)]$$

where for isotropic rotational-diffusive motion:

$$J(\omega) = \tau/[1+(\omega\tau)^2] \quad (3)$$

where $s_H = 1/2$, $s_D = 1$, and the diagonal elements are sums over the ρ_{H_iF} or $\rho_{H_iH_j}$ values. The diagonal elements of the resulting NOESY matrix are calculated using standard matrix-diagonalization procedures as described (e.g. by Gerig, 1980; Keepers and James, 1984; Massefski and Bolton, 1985), to obtain a NOESY intensity matrix, $\mathbf{A} = \exp[-\mathbf{R}\tau]\cdot\mathbf{A}_0$, where τ is the mixing time. The diagonal elements correspond to the spin-lattice relaxation of the nuclei, normalized to decay from 1.0 to 0, and the matrix is set up so that A_{11} corresponds to the fluorine nucleus. For an isolated ^{19}F-^{1}H spin pair with internuclear distance $r_{HF} = 2.5$ Å, assuming isotropic motion characterized by a correlation time $\tau_M = 23$ ns, a markedly nonexponential curve is obtained, corresponding to an initial decay of ~50% of the intensity, as the initial ^{19}F excitation is shared with the nearby proton (Fig. 2). The subsequent decay of the magnetization proceeds very slowly, requiring hundreds of seconds, since the spectral density components for this system corresponding to $\tau_M = 23$ ns do not provide an efficient pathway to the lattice. A second simulation shows the effects of having several protons arranged in a line, as illustrated in Fig. 2. In this case, the initial approximately exponential decay lasts until ~25% of the initial excitation remains. Thus, the effect of the large number of protons in the protein system essentially uncouples the relaxation behavior, so that a simple decay curve with a relaxation rate approximately equal to R_{11}, the first element of the relaxation matrix (see below), is obtained. This can be taken into account by using additional protons or, as illustrated by the dotted curve, by adding a proton-relaxation sink corresponding to a rate of 1 s^{-1}, as is typically invoked for protein systems (Ishima et al., 1991). Hence, the effect of the large number of protein spins combined with rapid spin diffusion is to uncouple the fluorine spin-lattice relaxation so that approximately exponential behavior is observed. Similar conclusions for fluorotyrosine-containing proteins have been derived by Hull and Sykes (1975a).

Based on the above discussion, the spin-lattice relaxation of the ^{19}F probe nucleus will be exponential, with a rate constant which is essentially a sum over all proton–fluorine dipolar interactions:

$$R_{1F}(H) = \sum_i \rho_{H_iF} \quad (4)$$

where the sum extends over all of the protons in the protein. For the ^{19}F nuclei in the deuterofluorotryptophan-labeled system, the corresponding fluorine spin-lattice relaxation rate will be given by:

$$R_{1F}(D) = \sum_{j=1}^{4}\rho_{D_jF} + \sum_{i'}\rho_{H_{i'}F} \quad (5)$$

where the index i' extends over all nondeuterated positions, and the index j extends over the four deuterated positions in the ring. In general, the first term on the right-hand side of Eq. 5 is negligible, so that:

$$R_{1F}(H) - R_{1F}(D) \approx \sum_{i=1}^{4}\rho_{H_iF} \quad (6)$$

where the summation above extends over the four protonated positions on the fluoroindole ring. We have thus neglected the rare complication arising when two fluorotryptophans are sufficiently close so that deuterons/protons on one residue make significant relaxation contributions to the ^{19}F on a second fluorotryptophan residue.

In order to account for internal motion of the tryptophan residues, we have utilized a 'model-free' approach designed to account for motional restriction by means of an order parameter S^2, and characteristic correlation times corresponding to overall and internal motion (Lipari and Szabo, 1982). The corresponding spectral density has the form:

$$J(\omega) = (1-S^2)\frac{\tau}{1+(\omega\tau)^2} + S^2\frac{\tau_M}{1+(\omega\tau_M)^2} \quad (7)$$

where the motion of the protein is assumed to be isotropic with a rotational correlation time τ_M, S^2 is the order parameter, the internal motion has a characteristic correlation time τ_i, and $\tau^{-1} = \tau_M^{-1} + \tau_i^{-1}$. Using the known internuclear distances in tryptophan, we can calculate $R_{1F}(H) - R_{1F}(D)$ by summing over the four substituted positions of the indole ring. As discussed above, a value of 23 ns for the rotational correlation time of the glucose–GGR complex was initially calculated using the average value

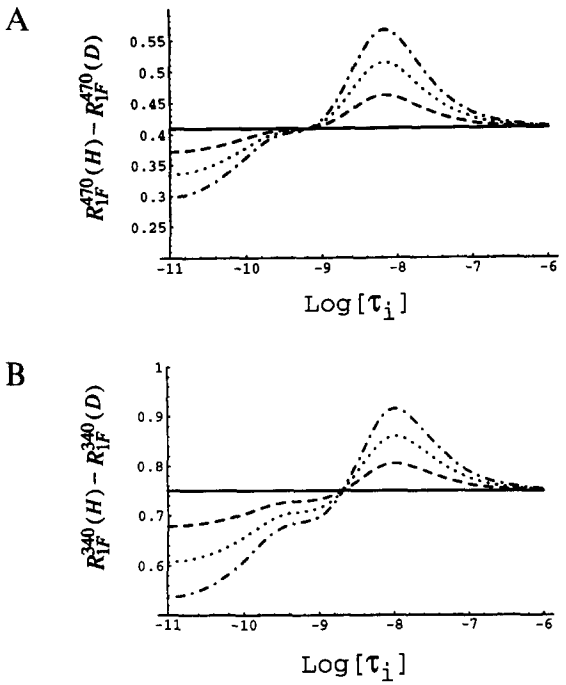

Fig. 3. Theoretical dependence of $R_{1F}(H)$–$R_{1F}(D)$, i.e., the difference in the spin-lattice relaxation rates between the fluorotryptophan and deuterated fluorotryptophan-labeled receptor, on the internal motional correlation time, τ_i, using a model-free formalism with $\tau_M = 23$ ns: (A) $H_o = 11.75$ T; (B) $H_o = 8.5$ T. Curves correspond to order parameters $S^2 = 1.0$ (——), 0.9 (– – –), 0.8 (· · · ·), or 0.7 (– · –). Relatively slow internal motions with correlation times ~ 10^{-8} s will increase $R_{1F}(H)$–$R_{1F}(D)$, while motions with shorter correlation times can lead to a decrease.

of $R_{1F}(H) - R_{1F}(D)$ for tryptophan residues 127, 133, 183, and 195, and assuming rigid, isotropic motion. FTrp[284] was omitted from this calculation since the spin-lattice relaxation rates for this residue are considerably longer, presumably reflecting a significant degree of internal motion. However, as is apparent from Table 1, including the values for this residue would not have a major impact on the computed averages. The 23-ns value corresponds to $R_{1F}(H) - R_{1F}(D) = 0.41$ s^{-1} at 470 MHz, and $R_{1F}(H) - R_{1F}(D) = 0.75$ s^{-1} at 340 MHz.

Using $\tau_M = 23$ ns and the model-free spectral density given above, theoretical curves for $R_{1F}(H) - R_{1F}(D)$ as a function of τ_i for values of the order parameter, $S^2 = 1.0$, 0.9, 0.8, and 0.7, are shown in Fig. 3. As can be seen from these curves, relatively low amplitude ($S^2 \sim 0.8$), slow ($\tau_i \sim 10^{-8}$–10^{-9} s) internal motion leads to significant increases in the differential spin-lattice relaxation rate, while faster internal motion reduces the relaxation rates relative to the $S^2 = 1.0$ case. As is apparent from the data in Table 1, the $R_{1F}(H) - R_{1F}(D)$ values show too much scattering to allow more explicit analysis. To the extent that a single order parameter model is appropriate to characterize the interresidue ^{19}F-^1H dipolar interactions, a similar set of curves will describe the individual $R_{1F}(H)$ values. The calculations shown in Fig. 3 suggest that, for a dominant dipolar relaxation mechanism, very different conclusions regarding the relationship of tryptophan order parameter to spin-lattice relaxation rate are derived, depending on the rates characterizing the internal motion. For internal motion characterized by relatively slow correlation times, i.e., $\tau_i \sim 10^{-8}$ s, we obtain higher relaxation rates for the less ordered (lower S^2) residues. Conversely, for internal motion characterized by shorter correlation times, $\tau_i \sim 10^{-10}$–10^{-11} s, we will obtain higher relaxation rates for the more ordered (higher S^2) tryptophan residues. Hence, if the differences observed among the various fluorotryptophan residues arise primarily as a consequence of variations in S^2, the residues with the highest relaxation rates, e.g. FTrp[183], would have the lowest order parameter for $\tau_i \sim 10^{-8}$ s, while the same residues would have the highest order parameter for $\tau_i \sim 10^{-11}$ s. As discussed below, internal motions at $\tau_i \sim 10^{-8}$ s appear to be inconsistent with relaxation-rate ratios measured at the two field strengths. Hence we conclude that, subject to the assumption that T_1 is dominated by dipolar ^1H-^{19}F interactions (Hull and Sykes, 1974), internal motion of the tryptophan residues must be characterized by high order parameters, and by relatively short internal correlation times, $\tau_i \sim 10^{-11}$ s.

Theoretical curves for the ratios of the relaxation rates measured at 8.5 and 11.75 T, $R_{1F}(H)^{340}/R_{1F}(H)^{470}$, have been calculated for the case of isotropic motion (Fig. 4A) or for the case of internal motion described by Eq. 7 (Fig.

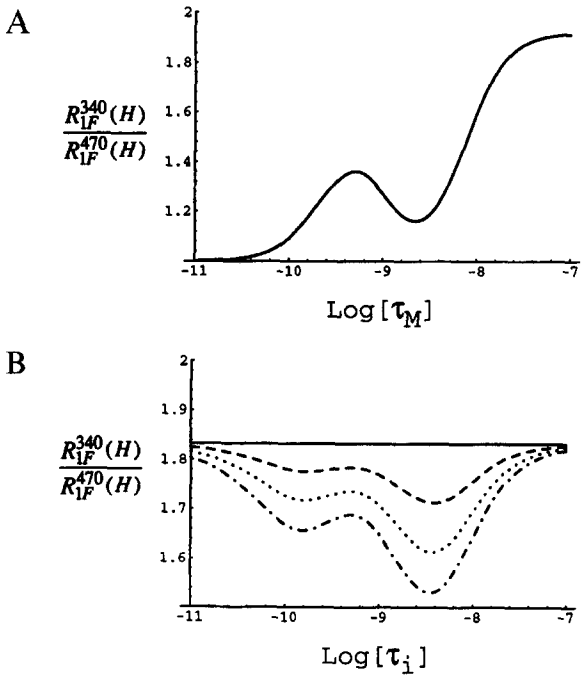

Fig. 4. Theoretical dependence of the ratio $R_{1F}(H)^{340}/R_{1F}(H)^{470}$ as a function of the correlation time for isotropic motion, τ_M (A), or as a function of the internal motional correlation time τ_i assuming $\tau_M = 23$ ns, and using a spectral density of the form of Eq. 7 (B). For the latter calculations, order parameter $S^2 = 1.0$ (——), 0.9 (– – –), 0.8 (· · · ·), or 0.7 (– · –). The calculations assume that the longitudinal relaxation occurs completely via a proton–fluorine dipolar mechanism.

TABLE 3
THEORETICAL ^1H-^{19}F DIPOLAR CONTRIBUTIONS TO ^{19}F SPIN-LATTICE RELAXATION RATES AND LINE WIDTHS BASED ON CRYSTAL DATA[a]

Residue	Spin-lattice relaxation rate (s^{-1})						$W_{1/2}$ (Hz)	
	470 MHz			340 MHz			470 MHz	340 MHz
	$^1H<3$ Å	$^1H<4$ Å	$^1H<5$ Å	$^1H<3$ Å	$^1H<4$ Å	$^1H<5$ Å		
Fluorotryptophan-labeled protein								
$FTrp^{183}$	1.79	1.95	2.09	3.28	3.57	3.83	25.6	25.8
$FTrp^{127}$	1.00	1.30	1.38	1.83	2.38	2.54	17.0	17.1
$FTrp^{133}$	1.26	1.47	1.59	2.31	2.69	2.91	19.4	19.6
$FTrp^{195}$	1.14	1.37	1.50	2.08	2.51	2.75	18.4	18.6
$FTrp^{284}$	0.61	0.69	0.79	1.12	1.26	1.44	9.6	9.7
[2,4,6,7-$^2H_4$]-5-Fluorotryptophan-labeled protein								
$FTrp^{183}$	1.27	1.43	1.56	2.34	2.62	2.86	19.1	19.3
$FTrp^{127}$	0.44	0.74	0.82	0.81	1.35	1.50	10.0	10.1
$FTrp^{133}$	0.72	0.92	1.03	1.31	1.69	1.89	12.6	12.8
$FTrp^{195}$	0.64	0.87	0.99	1.17	1.60	1.82	12.1	12.3
$FTrp^{284}$	0.09	0.16	0.25	0.16	0.30	0.47	3.1	3.1

[a] Computed relaxation times based on a correlation time of 23 ns, and no internal motion, i.e., $S^2 = 1.0$.

4B). Using the assumption of a dominant dipolar relaxation mechanism, the exact number or relative orientation of the various proton–fluorine interactions do not have to be determined, since the ratio is independent of these variables. Furthermore, since the fluorine–deuterium dipolar interaction is relatively weak, the curves should also be reasonable approximations for the following ratio: $R_{1F}(D)^{340}/R_{1F}(D)^{470}$. As noted above, similar relaxation-rate ratios are measured for both the deuterated and protonated fluorotryptophan residues. Based on the calculation shown in Fig. 4A, it is seen that close agreement with the experimental values is obtained for $\tau_M = 23$ ns ($\log[2.3 \times 10^{-8}\ s] = -7.64$). Considering the calculations of Fig. 3B, the observed field dependence of the T_1 values requires that either: (i) values of S^2 are very close to 1.0; and/or (ii) the correlation time for internal motion, τ_i, is very short, i.e., near 10^{-11} s.

In order to provide further insight into the relaxation differences between the various tryptophan residues of GGR, relaxation rates were determined based on the crystal structure of the glucose–GGR complex (Vyas et al., 1988). Starting with the structure of the glucose-complexed GGR, the H5 protons on each tryptophan were replaced by fluorine nuclei using standard bond and angle parameters from the CHARMm 22 force field ($r_{CF} = 1.338$ Å). Protons were grown onto the crystal structure using the standard CHARMm protocol, and the structure was minimized using 100 steps of steepest descent followed by conjugate gradients, until the gradient went below 0.6 kcal/mol. Relaxation rates were calculated assuming isotropic motion with $\tau_M = 23$ ns, including all protons within 3, 4, or 5 Å. The calculated relaxation rates are summarized in Table 3. As discussed by Post et al. (1984), the dipolar relaxation contributions of protons can be approximated by integrating the proton density $\rho(r)$ over the volume of a sphere starting at a lower limit of $r_{FH} = 2.6$ Å to infinity:

$$R_{1F} \propto \int_{2.6}^{\infty} \frac{\rho(r) 4\pi r^2}{r^6} dr \qquad (8)$$

Assuming $\rho(r)$ to be a constant, the approximation made by integrating out to 5 Å rather than infinity would correspond to 86% of the full relaxation contribution, so that the values in Table 3 represent a reasonable approximation. These calculations reproduce the observed trends well using only a simple isotropic diffusion model. This agreement, obtained by using only a single correlation time, suggests that the variation in $R_{1F}(H)$ values can arise due to the varying distances to nearby protons rather than as a consequence of a variation in internal mobility. Subtraction of the calculated dipolar line-width contributions from the observed values yields values of 34–42 Hz for FTrp residues 183, 127, and 195 (Table 2), which presumably arises from a combination of unresolved scalar coupling and chemical shift anisotropy broadening. The contributions of unresolved scalar coupling to the apparent ^{19}F NMR line widths of fluorinated residues will in general be reduced by the phenomenon of 'relaxation decoupling', with the rapid cross-relaxation rates of the protons leading to partial collapse of the multiplet structure (London, 1990; Harbison, 1993).

Relaxation by chemical shift anisotropy

As a consequence of the relatively large chemical shift range for fluorine, the chemical shift anisotropy relaxation mechanism can be significant (Hull and Sykes, 1975b). For the simple case of isotropic motion, the expressions for $1/T_{1F}^{CSA}$ and $1/T_{2F}^{CSA}$ are relatively simple:

$$\frac{1}{T_{1F}^{CSA}} = \frac{2}{15}\gamma_F^2 B_0^2 \Delta\sigma^2 \left(1+\frac{\eta^2}{3}\right) J(\omega) \quad (9)$$

and

$$\frac{1}{T_{2F}^{CSA}} = \frac{1}{45}\gamma_F^2 B_0^2 \Delta\sigma^2 \left(1+\frac{\eta^2}{3}\right) [4J(0)+3J(\omega)] \quad (10)$$

where as above, $J(\omega) = \tau/(1+(\omega\tau)^2)$ for isotropic motion, $\Delta\sigma = \sigma_{zz} - 1/2(\sigma_{xx}+\sigma_{yy})$, and $\eta = (\sigma_{xx}-\sigma_{yy})/\sigma_{zz}$, and we have followed the conventions: $|\sigma_{zz}| \geq |\sigma_{xx}| \geq |\sigma_{yy}|$, $\sigma_{zz}+\sigma_{xx}+\sigma_{yy}=0$. Hiyama et al. (1986) have studied crystalline *p*-fluoro-D,L-phenylalanine, which might be considered as a reasonable model for aromatic fluorine shift anisotropy. Elements of the chemical shift tensor (using the above conventions) are $\sigma_{zz} = -66.67$ ppm, $\sigma_{xx} = 58.33$ ppm, and $\sigma_{yy} = 8.33$ ppm, giving $\Delta\sigma = -100$ ppm, $\eta = 0.75$, and $\Delta\sigma(1+(\eta^2/3))^{1/2} = -109$ ppm. Other relevant measurements include the values reported for fluorobenzene (Mehring et al., 1976): $\sigma_{zz} = -58$, $\sigma_{yy} = 7$, $\sigma_{xx} = 51$ ppm, leading to $\Delta\sigma = -87$ ppm; $\eta = 0.76$, giving $\Delta\sigma(1+(\eta^2/3))^{1/2} = -95$ ppm, as well as measurements on crystalline 4,4'-difluorobiphenyl (Halstead et al., 1976) giving $\sigma_{zz} = -54.93$ ppm, $\sigma_{xx} = 51.77$ ppm, and $\sigma_{yy} = 3.17$ ppm, corresponding to $\Delta\sigma(1+(\eta^2/3))^{1/2} = -92.5$ ppm.

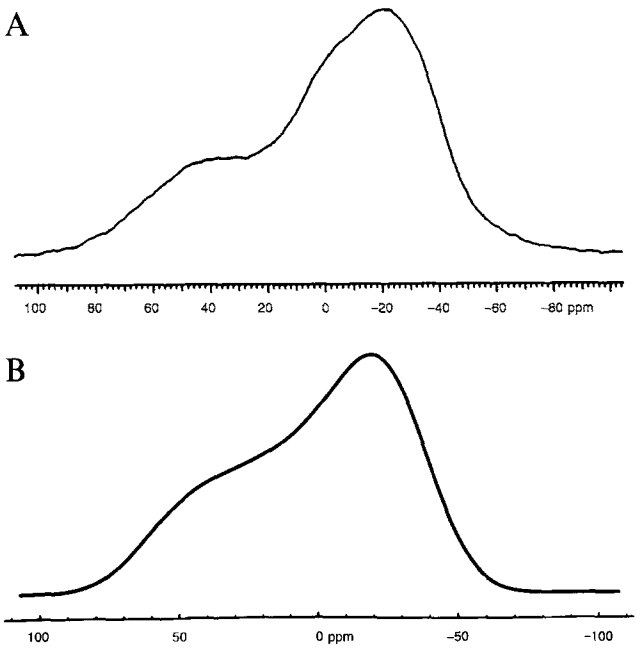

Fig. 5. (A) Solid-state ^{19}F NMR spectrum of a powder sample of [2,4,6,7-$^2H_4$]-D,L-5-fluorotryptophan obtained using a spin-echo sequence. A spectral window of 100 kHz (213 ppm), and a 0.01 s acquisition time were used. A total of 360 FIDs were averaged, left-shifted three points to center the echo about the time origin, and phased such that the real and imaginary components were purely absorptive and dispersive, respectively. An exponential apodization of 1 kHz was applied to the FID prior to Fourier transformation. No further phasing was applied in the frequency domain. The spectrum is referenced to the ^{19}F shift of the molecule in the liquid state. (B) Theoretical curve generated using the intensity pattern for an axially symmetric shift tensor convoluted with a Gaussian function. The theoretical curve corresponds to $\Delta\sigma(1+(\eta^2/3))^{1/2} = -94$ ppm ($\sigma_{xx} = 38.7$ ppm, $\sigma_{yy} = 23.7$ ppm, $\sigma_{zz} = -62.3$ ppm).

In order to obtain a more quantitative estimate of the relaxation contributions due to chemical shift anisotropy, direct measurements of the ^{19}F chemical shift tensor were carried out on [2,4,6,7-$^2H_4$]-D,L-5-fluorotryptophan. As in the previous study of deuterated 4-fluorophenylalanine (Hiyama et al., 1986), the deuteration is useful in reducing the ^1H-^{19}F static dipolar contributions so that the lineshape is dominated by the orientation-dependent shift tensor. The resulting solid-state spectrum (Fig. 5A) appears to be more axially symmetric than the 4-fluorophenylalanine spectrum. A simulation of the solid-state spectrum convoluted with a Gaussian broadening function using parameters $\sigma_{zz} = -62.3$ ppm, $\sigma_{yy} = 23.7$ ppm, $\sigma_{xx} = 38.7$ ppm, corresponding to $\Delta\sigma = -93.5$ ppm; $\eta = 0.24$, giving $\Delta\sigma(1+(\eta^2/3))^{1/2} = -94$ ppm is shown in Fig. 5B. Although the simulation is reasonably close, the dip in the center of the spectrum is not well predicted. This may arise from a pulsing artifact (Rance and Byrd, 1983). It is also apparent from Fig. 5 that the deuteration of the indole ring is insufficient to remove much of the dipolar broadening. The value obtained for $\Delta\sigma(1+(\eta^2/3))^{1/2}$ is, however, in good agreement with the model compounds noted above.

Using values of $\Delta\sigma(1+(\eta^2/3))^{1/2} = -94$ ppm, and a rotational correlation time of 23 ns in the above equations, we obtain 0.051 s^{-1} for R_{1F}^{CSA} at either field, and line-width contributions ($1/\pi T_2^{CSA}$) of 50.2 and 26.2 Hz at 11.75 and 8.5 T, respectively. This spin-lattice relaxation rate is much lower than the observed values or the theoretical dipolar values, indicating that, if isotropic motion is assumed, the CSA mechanism is not significant relative to the dipolar mechanism. However, the CSA line-width contribution is too large to fit the experimental values determined at 470 MHz (Table 2) using the rigid, isotropic motion model. As discussed below, this discrepancy is resolved by using the more complex spectral density described by Eq. 7. The negligible contribution of CSA to R_{1F} compared with the dipolar contribution arises due to the presence in the dipolar-rate equation of $J(\omega_F - \omega_H)$, which is significantly larger than $J(\omega_F)$ for the slower motion which characterizes overall protein tumbling.

Following the above approach, we have used the model-free spectral density to evaluate the effects of internal motion on the CSA relaxation parameters. Calculations of R_{1F}^{CSA} and $W_{1/2}^{CSA}$ for a field strength of 11.75 T using a model-free spectral density with $\Delta\sigma(1+(\eta^2/3))^{1/2} = -94$ ppm are shown in Fig. 6. Although the contributions of the CSA mechanism to R_{1F} are seen to be negligible for slow, isotropic motion, the contributions become more significant for internal correlation times, τ_i, closer to $1/\omega_F = 3.4 \times 10^{-10}$ s. For fast internal motions described by correlation times $\tau_i \leq 10^{-9}$ s, the resonance half widths are re-

duced by a factor of S^2, i.e., $W_{1/2} \approx S^2 W^0_{1/2}$, where $W^0_{1/2}$ is the line width at half height in the absence of internal motion. These results suggest that an improved fit of the relaxation data can be achieved based on the assumption of very fast internal motion, $\tau_i \leq 10^{-11}$ s, and order parameters near 1 in order to exert minimal perturbation of the dipolar-dominated spin-lattice relaxation, while leading to a reduced, $S^2 W^0_{1/2}$, line width.

As a final theoretical tool, calculations including both dipolar and CSA relaxation contributions were performed. In order to evaluate the combined effects of both relaxation mechanisms, the proton–fluorine dipolar interaction was approximated by a single proton located 1.8 Å from the fluorine nucleus and, based on the solid-state data, $\Delta\sigma(1+(\eta^2/3))^{1/2} = -94$ ppm. The theoretical $R_{1F}(H)^{470}$, $W_{1/2}$, and $R_{1F}(H)^{340}/R_{1F}(H)^{470}$ are plotted using a model-free formalism and S^2 values of 1.0, 0.9, 0.8, and 0.7 (Fig. 7). The calculated dependence of $R_{1F}(H)^{470}$ is qualitatively similar to the calculation for $R_{1F}(H)^{470} - R_{1F}(D)^{470}$. The curves for $W_{1/2}$ show the same dependence on τ_i as the CSA calculation (Fig. 6B), while the curve for the ratio of relaxation rates, $R_{1F}(H)^{340}/R_{1F}(H)^{470}$, exhibits an even more pronounced dip for τ_i values in the range from 10 ns to 100 ps. Although, as discussed below, the parameters for this model calculation do not provide an ideal fit of the data, Fig. 7C makes it even more clear that in order to reproduce the observed mean relaxation ratios, τ_i must be ≤ 10 ps.

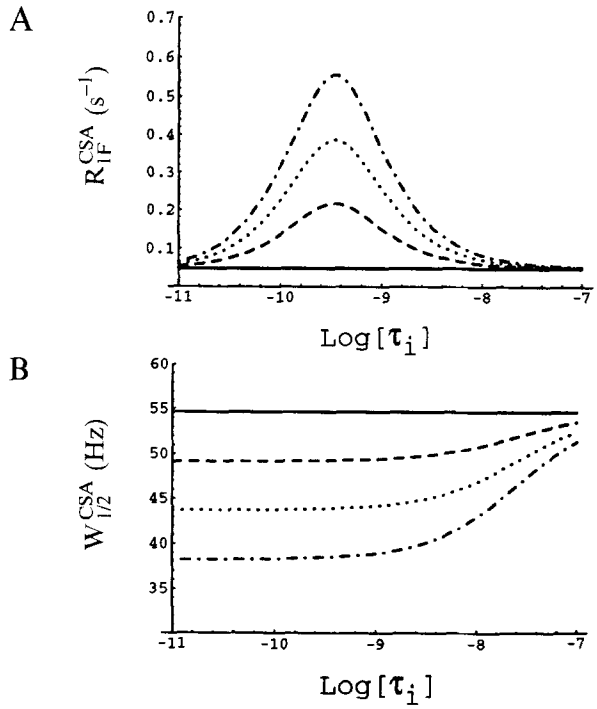

Fig. 6. The effects of internal motion on the spin-lattice relaxation rate R_{1F}^{CSA} (in s^{-1}) (A), and the line width $W_{1/2}^{CSA}$ (in Hz) (B), resulting from a chemical shift anisotropy relaxation mechanism. Calculations are based on a model-free spectral density using parameters $\Delta\sigma(1+(\eta^2/3))^{1/2} = -94$ ppm and $\tau_M = 23$ ns, and correspond to order parameters $S^2 = 1.0$ (——), 0.9 (– – –), 0.8 (· · · ·), or 0.7 (– · –). As is apparent from the figure, internal motion with a correlation time $\sim \tau_i = 10^{-9}$ s to 10^{-10} s can greatly increase the CSA contribution to R_1.

Refinement of dynamic variables

In order to obtain a consistent set of dynamic variables, τ_i was set at 10 ps, a typical value characterizing the motions of protein backbone nuclei (Kay et al., 1989; Cheng et al., 1994) or large side chains such as phenylalanine or tryptophan (Stone et al., 1993; Mispelter et al., 1995), and consistent with the qualitative analyses summarized above. The values of τ_M and S^2 were allowed to vary in order to simultaneously optimize the fit for the experimental parameters: $R_{1F}(H)^{470} - R_{1F}(D)^{470} = 0.39$ s^{-1}, $R_{1F}(H)^{340} - R_{1F}(D)^{340} = 0.79$ s^{-1}, and a mean chemical shift anisotropy line width of 37.5 Hz (Table 2); by minimizing the error function defined in the Methods (Eq. 1). As noted above, the relaxation behavior of $FTrp^{284}$, which exhibits significantly different relaxation parameters, was analyzed separately (see below), and the dipolar line-width contribution was fixed at the theoretical value estimated for $\tau_M = 23$ ns. The optimal fit, corresponding to the average values for the parameters given above, is obtained at $\tau_M = 20$ ns, $S^2 = 0.86$, and corresponds to parameter values of 0.40 s^{-1}, 0.73 s^{-1}, and 37.6 Hz, respectively. The computed ratio, $R_{1F}(H)^{340}/R_{1F}(D)^{470} = 1.80$, is also in good agreement with experiment. The computed error function was found to be fairly insensitive to the value of τ_i. The shorter correlation time, τ_M, obtained from this fitting procedure approximately corresponds to displacing the series of theoretical curves in Figs. 3A and 3B upward, so that instead of the optimized fit corresponding to $\tau_M = 23$ ns, $S^2 = 1.0$, the optimal fit obtained corresponds to $\tau_M = 20$ ns, $S^2 = 0.89$. Similarly, the set of curves in Fig. 7A will be displaced upward, while the curves in Fig. 7B will be displaced downward. Thus, while decreasing τ_M and S^2 lead to an approximate cancellation of effects on the R_{1F} values, the adjusted parameters correspond to a narrower line width, in agreement with the data in Table 2.

As a further attempt to more accurately account for the dipolar line-width contribution, the mean CSA line widths for the protonated and deuterated fluorotryptophans were obtained by subtracting dipolar line-width contributions of $S^2 W^{23}_{1/2}(\tau_M/23)/0.86$, where the initially calculated dipolar line width corresponding to a correlation time of 23 ns, $W^{23}_{1/2}$, is corrected by the ratio $\tau_M/23$ (in ns), based on the assumption of a dominant J(0) contribution, reduced by a factor of S^2 as would be expected for rapid internal motion, and the factor of 0.86 is included to correct for protons beyond the limit of 5 Å used in the calculations of Tables 2 and 3. It is undoubtedly incorrect to model all proton–fluorine dipolar interactions using the same order parameter; however, since the dipolar line-width contribution is significantly smaller than the CSA contribution, this was thought to be a

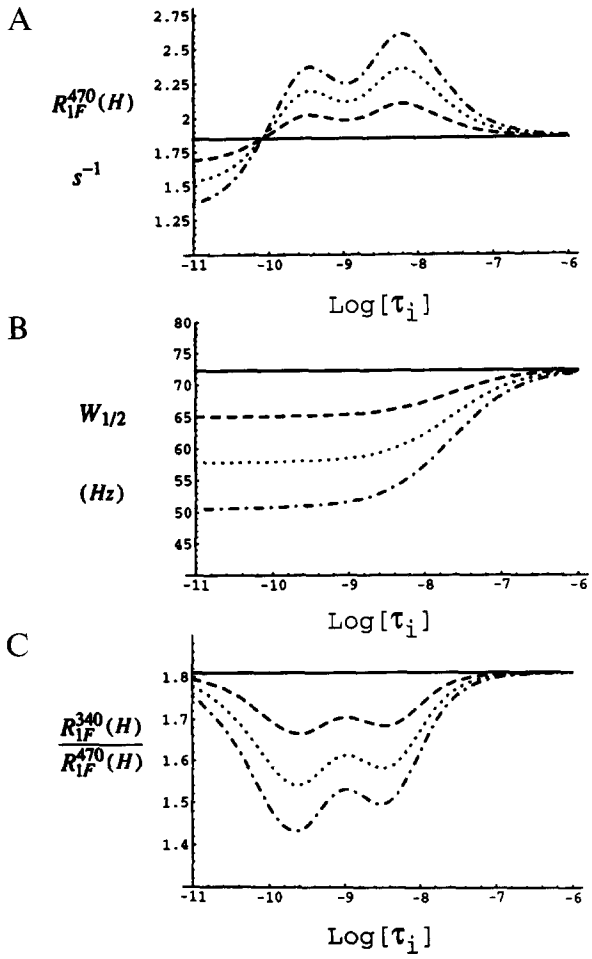

Fig. 7. Calculated relaxation parameters for a model including both dipolar and CSA effects. In order to approximate the dipolar contributions, the calculation assumes a single proton at a distance of 1.8 Å from the fluorine nucleus; other parameters are $\tau_M = 23$ ns, $\Delta\sigma(1 + (\eta^2/3))^{1/2} = -94$ ppm. This approximation yields rates that are roughly comparable to the observed values summarized in Table 1. (A) $R_{1F}(H)^{470}$ (s^{-1}); (B) $W_{1/2}$ (Hz); (C) $R_{1F}(H)^{340}/R_{1F}(H)^{470}$. Calculations correspond to order parameters $S^2 = 1.0$ (——), 0.9 (– – –), 0.8 (· · · ·), or 0.7 (– · –).

reasonable approximation. Following this procedure led to the values $\tau_M = 20$ ns, and $S^2 = 0.89$, corresponding to relaxation parameter values of 0.42 s^{-1}, 0.75 s^{-1}, and 38.9 Hz. Hence, both approaches gave similar values for τ_M and S^2.

Using the procedure outlined above, a separate analysis of the $FTrp^{284}$ relaxation data was performed. Setting $\tau_i = 10$ ps and $\tau_M = 20$ ns yielded a value of $S^2 = 0.77$, corresponding to computed relaxation parameter values of 0.36 s^{-1}, 0.65 s^{-1}, and a CSA line width of 33.6 Hz. Allowing τ_M to vary leads to a value of 19 ns, with S^2 still optimized at 0.77, resulting in a significant drop in the computed error. However, it seems more reasonable to constrain τ_M to the value determined using the less mobile fluorotryptophan residues. Hence, as expected, this residue located on the surface of the protein is significantly more disordered than the other fluorotryptophans.

Effect of glucose complexation

Although the ^{19}F NMR spectrum of the doubly labeled fluorotryptophan/deuterofluorotryptophan protein was found to be too congested for useful analysis, ^{19}F spin-lattice relaxation rates determined for the 5-fluorotryptophan-labeled GGR in both the glucose-complexed and -uncomplexed states were obtained, and the results are summarized in Table 4. As is apparent from a comparison with the data in Table 1, the R_{1F} values obtained in the fluorotryptophan-labeled GGR are found to be in good agreement with those measured in the doubly labeled protein. In the absence of glucose, the R_{1F} values for residues 183, 127, 133, and 195 decrease by a mean of 13%, while the R_{1F} value for $FTrp^{284}$ increases by 16%. Three of the residues, $FTrp^{127}$, $FTrp^{133}$, and $FTrp^{195}$, are located in one of the two lobes of the protein; $FTrp^{183}$ is located very close to the bound glucose at the interface of the two lobes of the protein, and $FTrp^{284}$ is located in the 'hinge' region connecting the two lobes. In the uncomplexed state, the enzyme conformation is characterized by a large, open cleft, with an angle ≥ 18° (Luck and Falke, 1991c). It might be expected that the local environment of the three residues located in one of the protein lobes would be relatively unchanged, so that the primary difference would be the effect on the overall motion of the protein. The conformational change associated with the aporeceptor would be expected to increase the radius of gyration, leading to a longer correlation time for overall tumbling. An increase of τ_M by 13% would be sufficient to explain the observed R_{1F} decreases for $FTrp^{127}$, $Ftrp^{133}$, and $FTrp^{195}$. Although $FTrp^{183}$ experiences a similar change in spin-lattice relaxation rate, this may be somewhat coincidental, since it is clear that in addition to any change in molecular correlation time there must be a significant change in the local environment of this residue.

The increased $R_{1F}(H)^{470}$ value for $FTrp^{284}$ observed in the uncomplexed protein (Table 4) indicates that, in addition to the increase in the correlation time for overall molecular motion, there is a significant change in local environment of this residue. This result is perhaps not too

TABLE 4
EFFECT OF GLUCOSE BINDING ON 5FTrp SPIN-LATTICE RELAXATION RATES IN THE *E. coli* GLUCOSE/GALACTOSE RECEPTOR[a]

Residue	Glc–GGR[b]	Glc–GGR[c]	GGR[d]
$FTrp^{183}$	1.91	1.89	1.41
$FTrp^{127}$	1.34	1.39	1.26
$FTrp^{195}$	1.40	1.47	1.27
$FTrp^{133}$	1.35	1.26	1.24
$FTrp^{284}$	0.95	0.93	1.09

[a] Spin-lattice relaxation rates determined at 470 MHz, 25 °C.
[b] Measurements on the 50:50 5FTrp:[2,4,6,7-$^2H_4$]-5FTrp-labeled GGR–glucose complex, taken from Table 1.
[c] Measurements on 5FTrp-labeled GGR.
[d] Measurements on uncomplexed GGR.

surprising, since this residue is located in the 'hinge' region of the protein. Since in this case we have not been able to separate intra- from interresidue dipolar relaxation contributions, it is also difficult to separate structural from dynamic changes. Movement of $FTrp^{284}$ away from nearby residues on the protein could contribute to the observed increase in R_{1F}. Although overlap of the $FTrp^{284}$ and $FTrp^{133}$ resonances makes quantitation difficult, it appears that there is no major change in line width. The simplest approach for predicting the observed increase in R_{1F} within the context of the present model, while retaining a similar line width, is to increase τ_t. For the parameters given above, i.e., $\tau_M = 20$ ns, $S^2 = 0.77$, and $\tau_i = 10$ ps, the CSA mechanism contributes 7%, the intraresidue dipolar mechanism 39%, and the interresidue dipolar interaction 54% to the observed $R_{1F}(H)$ for the glucose–GGR complex. Assuming the intra/interresidue dipolar ratio to be fixed, increasing τ_M by 13% requires that τ_i increase from 10 to 70 ps, and that S^2 decrease from 0.77 to 0.67 in order to predict the observed R_{1F} change and preserve the CSA line-width contribution. For these parameters, the CSA contribution to R_{1F} has increased to 24%. In general, more extensive relaxation data are required in order to adequately separate structural and dynamic changes which occur in the uncomplexed GGR.

Discussion and Conclusions

Fluorine labeling of macromolecules provides an NMR probe of high sensitivity, with potential applicability to high molecular weight systems. Assignment strategies have become more straightforward, based on the use of site-directed mutagenesis (Jarema et al., 1981; Ho et al., 1989; Li et al., 1989; Peersen et al., 1990; Luck and Falke, 1991a). In general, fluorinated proteins possess similar structural and kinetic properties to the native forms, so that in most cases the relatively small number of fluorinated residues and low specific enrichment of each position limit the perturbation introduced. In general, it might be argued that if a fluorinated amino acid analog located at a particular position in the protein exerts a significant destabilizing effect, the correspondingly labeled proteins will be more subject to denaturation. In this case, one might expect to observe variations in the fluoro-amino acid substitution level at different positions in the molecule. However, this has not been observed in the present GGR studies, and appears not to be the case generally. Conversely, it is conceivable that the fluorine substituent could introduce a significant stabilization corresponding to a particular fluorotryptophan substitution site. The slightly greater incorporation observed at the $FTrp^{127}$ position may arise from such an effect; however, the fractional increase in resonance intensity relative to the other FTrp residues is within the experimental error.

The present studies were undertaken to evaluate the utility of fluorinated amino acids for dynamic characterization of large proteins. In contrast to the smaller proteins which are often the objects of ^1H NMR studies, the long correlation times associated with overall tumbling of fluorine-labeled molecules renders the spin-lattice relaxation relatively insensitive to overall molecular tumbling, enhancing the relative sensitivity to internal motion. One particular limitation on the use of fluorinated amino acids as dynamic probes arises as a consequence of the varied contributions to spin-lattice relaxation. Consistent with and extending the earlier conclusions of Hull and Sykes (1974,1975a,b), evaluation of the data for fluorotryptophan-labeled GGR indicates that: (i) ^1H-^{19}F dipolar interactions dominate the observed spin-lattice relaxation rates, even at high field strengths; and (ii) both intra- and interresidue interactions are significant. The latter factor makes dynamic analysis particularly difficult, since these interactions may be characterized by very different internal motional correlation times and order parameters. The use of simultaneous fluorotryptophan/deuterofluorotryptophan labeling provides a useful means of separating intra- and interresidue effects, since the difference in relaxation rates will depend only on the motion of the indole ring. Unfortunately, the experimental variation in $R_{1F}(H) - R_{1F}(D)$ rates in this study proved sufficiently large so that conclusions were derived only for average values rather than for the individual residues, with the exception of $FTrp^{284}$, which exhibited markedly different relaxation behavior. It is in principle also possible to separate the intraresidue contribution to the transverse relaxation rate, $R_{2F}(H) - R_{2F}(D)$; however, this presents a more difficult problem since it will correspond to a small difference between large values due to the dominant CSA contribution to the transverse relaxation rate.

Simulations of the various relaxation parameters using the model-free spectral density approach indicate that internal motions with slow correlation times $\sim 10^{-8}$ s are inconsistent with the observed relaxation parameters. For example, the theoretical ratio $R_{1F}^{340}/R_{1F}^{470}$ corresponding to $\tau_i = 10$ ns falls significantly below the experimental values: $R_{1F}(H)^{340}/R_{1F}(H)^{470} = 1.86$, and $R_{1F}(D)^{340}/R_{1F}(D)^{470} = 1.81$, even for order parameters near 1.0 (Figs. 4B and 7C). This discrepancy becomes even more significant if the spin-lattice relaxation contribution due to CSA relaxation is included in the calculation (data not shown). Similar conclusions regarding the absence of significant internal motions with correlation times ~ 10 ns have been derived from studies of 5-fluorotryptophan-labeled histidine-binding protein J of *S. typhimurium* (Post et al., 1984). Instead, internal motion consistent with the observed relaxation behavior must be characterized by high order parameters and relatively short correlation times, ~ 10 ps. These correlation times are similar to values recently reported for the peptide backbone of small proteins (Kay et al., 1989; Cheng et al., 1994), and for the internal motion of trypto-

phan residues of thioredoxin (Stone et al., 1993) and aponeocarzinostatin (Mispelter et al., 1995). In this limit, initially discussed by Marshall et al. (1972), the calculated relaxation parameters become nearly independent of the value of τ_i. Further analyses of the data were based on setting $\tau_i = 10$ ps, using $\Delta\sigma(1-(\eta^2/3))^{1/2} = -94$ ppm, as determined from solid-state NMR lineshape analysis, and varying τ_M and S^2 to obtain an optimal fit of the parameters $R_{1F}(H)^{470} - R_{1F}(D)^{470}$, $R_{1F}(H)^{340} - R_{1F}(D)^{340}$, and $W_{1/2}^{470}$. An average order parameter of 0.89 was obtained for FTrp residues 127, 133, 183, and 195, while a value of 0.77 was obtained for $FTrp^{284}$. These values compare well with order parameter values of 0.91 and 0.93 for the buried tryptophan residue 28 of oxidized or reduced thioredoxin, and values of 0.82 and 0.81 for the surface Trp^{31} of the same protein (Stone et al., 1993). Similarly, order parameter values ranging from 0.85 to 0.97 with a mean of 0.92 have been reported for the five tryptophan residues of *E. coli* dihydrofolate reductase (Epstein et al., 1995). A value of $S^2 = 0.83$ is reported for Trp^{83} of aponeocarzinostatin (Mispelter et al., 1995). Interestingly, there is no indication of significant conformational exchange broadening for the fluorotryptophan resonances of glucose-complexed GGR.

In addition to the data on the fluorotryptophan/deuterofluorotryptophan R_{1F} differences, there is significant variation among the tryptophan $R_{1F}(H)$ values. The general trend observed, $R_{1F}^{183} > R_{1F}^{127} \sim R_{1F}^{133} \sim R_{1F}^{195} > R_{1F}^{284}$ is found to be predicted based on the distribution of protons near the fluorine nuclei, derived from the crystal-structure data (Vyas et al., 1988). Although this result suggests that dynamic variations are not necessarily responsible for the observed pattern, it is interesting to note that the corresponding isotropic B-factors for the tryptophan side chains listed in the same order are: 7.88, 14.57, 15.99, 13.35, and 22.36, respectively. Thus, the B-factors follow the pattern: $B^{183} < B^{127} \sim B^{133} \sim B^{195} < B^{284}$. This inverse correlation of the fluorine spin-lattice relaxation rates with the crystallographic B-factors is consistent with the conclusion that dynamic variations might also contribute to the observed R_{1F} variation.

Glucose binding is associated with significant changes in the R_{1F} values of the fluorotryptophan residues. In the absence of glucose, the R_{1F} values for residues 183, 127, 133, and 195 decrease by a mean of 13%, while the R_{1F} value for $FTrp^{284}$ increases by 16%. These changes are consistent with an increase in the correlation time for overall molecular tumbling, combined with a change in the internal mobility in the hinge region of the protein. Although the absence of more extensive data for the uncomplexed receptor limits the conclusions, it appears that increased disorder, with $S^2 = 0.67$, and slower internal motion with a correlation time $\tau_i \sim 70$ ps can explain the observed data. In general, more extensive relaxation measurements are required to separate structural and dynamic changes in the uncomplexed receptor.

References

Ando, M.E., Gerig, J.T. and Luk, K.F.S. (1986) *Biochemistry*, **25**, 4772–4778.

Browne, D.T. and Otvos, J.D. (1976) *Biochem. Biophys. Res. Commun.*, **68**, 907–913.

Cheng, J.-W., Lepre, C.A. and Moore, J.M. (1994) *Biochemistry*, **33**, 4093–4100.

Epstein, D.M., Benkovic, S.J. and Wright, P.E. (1995) *Biochemistry*, **34**, 11037–11048.

Gerig, J.T. (1980) *J. Am. Chem. Soc.*, **102**, 7308–7312.

Gerig, J.T., Klinkenborg, J.C. and Nieman, R.A. (1983) *Biochemistry*, **22**, 2076–2087.

Gerig, J.T. (1994) *Prog. NMR Spectrosc.*, **26**, 293–370.

Griffiths, D.V., Feeney, J., Roberts, G.C.K. and Burgen, A.S.V. (1976) *Biochim. Biophys. Acta*, **446**, 479–485.

Halstead, T.K., Speiss, H.W. and Haeberlen, U. (1976) *Mol. Phys.*, **31**, 1569–1583.

Harbison, G.S. (1993) *J. Am. Chem. Soc.*, **115**, 3026–3027.

Hinds, M.G., King, R.W. and Feeney, J. (1992) *Biochem. J.*, **287**, 627–632.

Hiyama, Y., Silverton, J.V., Torchia, D.A., Gerig, J.T. and Hammond, S.J. (1986) *J. Am. Chem. Soc.*, **108**, 2715–2723.

Ho, C., Pratt, E.A. and Rule, G.S. (1989) *Biochim. Biophys. Acta*, **988**, 173–184.

Hoeltzli, S. and Frieden, C. (1994) *Biochemistry*, **33**, 5502–5509.

Hull, W.E. and Sykes, B.D. (1974) *Biochemistry*, **13**, 3431–3437.

Hull, W.E. and Sykes, B.D. (1975a) *J. Chem. Phys.*, **63**, 867–880.

Hull, W.E. and Sykes, B.D. (1975b) *J. Mol. Biol.*, **98**, 121–153.

Ishima, R., Shibata, S. and Akasaka, K. (1991) *J. Magn. Reson.*, **91**, 455–465.

Jarema, M.A., Lu, P. and Miller, J.H. (1981) *Proc. Natl. Acad. Sci. USA*, **78**, 2707–2711.

Kay, L.E., Torchia, D.A. and Bax, A. (1989) *Biochemistry*, **28**, 8972–8979.

Keepers, J.W. and James, T.L. (1984) *J. Magn. Reson.*, **57**, 404–426.

Li, E., Qian, S., Nader, L., Yang, N.C., d'Avignon, A., Sacchettini, J.C. and Gordon, J.I. (1989) *J. Biol. Chem.*, **264**, 17041–17048.

Lipari, G. and Szabo, A. (1982) *J. Am. Chem. Soc.*, **104**, 4546–4559.

London, R.E. (1990) *J. Magn. Reson.*, **86**, 410–415.

Luck, L.A. and Falke, J.J. (1991a) *Biochemistry*, **30**, 4248–4256.

Luck, L.A. and Falke, J.J. (1991b) *Biochemistry*, **30**, 4257–4261.

Luck, L.A. and Falke, J.J. (1991c) *Biochemistry*, **30**, 6484–6490.

Marshall, A.G., Schmidt, P.G. and Sykes, B.D. (1972) *Biochemistry*, **11**, 3875–3879.

Massefski Jr., W. and Bolton, P.H. (1985) *J. Magn. Reson.*, **65**, 526–530.

Matthews, H.R., Matthews, K.S. and Opella, S.J. (1977) *Biochim. Biophys. Acta*, **497**, 1–13.

Mehring, M. (1976) In *NMR: Basic Principles and Progress*, Vol. 11 (Eds, Diehl, P., Fluck, E. and Kosfeld, R.), Springer, Berlin, pp. 174–183.

Mispelter, J., Lefevre, C., Adjadj, E., Quiniou, E. and Favaudon, V. (1995) *J. Biomol. NMR*, **5**, 233–244.

Moreland, C.G. and Carroll, F.I. (1974) *J. Magn. Reson.*, **15**, 596–599.

Morris, G.A. and Freeman, R. (1978) *J. Magn. Reson.*, **29**, 433–462.

Osten, H.J., Jameson, C.J. and Craig, N.C. (1985) *J. Chem. Phys.*, **83**, 5434–5441.

Peersen, O.B., Pratt, E.A., Truong, H.-T.N., Ho, C. and Rule, G.S. (1990) *Biochemistry*, **29**, 3256–3262.

Post, J.F.M., Cottam, P.F., Simplaceanu, V. and Ho, C. (1984) *J. Mol. Biol.*, **179**, 729–743.

Rance, M. and Byrd, R.A. (1983) *J. Magn. Reson.*, **52**, 221–240.

Stone, M.J., Chandrasekhar, K., Holmgren, A., Wright, P.E. and Dyson, H.J. (1993) *Biochemistry*, **32**, 426–435.

Vyas, N.K., Vyas, M.N. and Quiocho, F.A. (1988) *Science*, **242**, 1290–1295.